BALKANTRIB'O5
5th INTERNATIONAL CONFERENCE ON TRIBOLOGY
JUNE.15-18. 2005
Kragujevac, Serbia and Montenegro

LOADING SIMULATION OF LUMBAR SPINE VERTEBRAE DURING A COMPRESSION TEST USING THE FINITE ELEMENTS METHOD AND TRABECULAR BONE STRENGTH PROPERTIES, DETERMINED BY MEANS OF NANOINDENTATIONS

K.-D. Bouzakis[1], S. Mitsi[1], N. Michailidis[1], I. Mirisidis[1], G. Mesomeris[1], G. Maliaris[1], A. Korlos[1], G. Kapetanos[2], P. Antonarakos[2], K. Anagnostidis[2]
1. Laboratory for Machine Tools and Manufacturing Engineering, Mechanical Engineering Department;Aristoteles University of Thessaloniki, Greece
2. 3rd Orthopaedic Department, "Papageorgiou" General Hospital, Medical School, Aristoteles University of Thessaloniki, Greece

Abstract
The mechanical strength properties of lumbar spine vertebrae are of great importance in a wide range of applications. Herein, through nanoindentations and appropriate evaluation of the corresponding results, trabecular bone struts stress–strain characteristics can be determined. In the frame of the present paper, an L2 fresh cadaveric vertebra, from which posterior elements were removed, was subjected to compression. With the aid of developed finite elements method based algorithms, the cortical shell and the cancellous core bulk elasticity moduli and stresses were determined, whereas the tested vertebra geometrical model used in these algorithms was considered having a compound structure, consisting of the cancellous bone surrounded by the cortical shell. Moreover nanoindentations were conducted and an appropriate evaluation method of the obtained results was applied to extract stress-strain curves of individual lumbar spine vertebra trabecular bone struts. These data were used in the mathematical description of the vertebra compression test. The vertebral cancellous bone structure was simulated by a beam elements network, possessing an equivalent porosity and different stiffnesses in vertical and horizontal direction. Thus the measured course of the compression load versus the occurring specimen deformation was verified.

Keywords: *Vertebrae Compression Test, Nanoindentation, Stress-strain Curves, Apparent Strength, Trabecular Bone Struts, Mechanical Properties*

1. INTRODUCTION

Up to now the mechanical properties of bones are determined by means of simple tension or compression tests [1,2] on unique material specimens with preformed dimensions as described in numerous publications.

In order to enable the determination of the elastic–plastic deformation behaviour of the various materials included in the structure of a

lumbar spine vertebra, such as of the cortical shell and the cancellous bone by means of compression tests directly on entire vertebra, an experimental-analytical procedure based on Finite Elements Method (FEM) simulations of the test and the specimens was developed.

The detected bulk material properties in the case of cancellous bone have to be considered as apparent ones, due to the fact that they do not correspond to individual structural components as, for example, to trabecular bone struts. Aiming to determine trabecular bone struts stress–strain curves, nanoindentation techniques were applied [3-5]. The obtained data were taken into account in the FEM simulation of a cancellous bone structure by means of an appropriate network of beam elements.

In this way a compression test diagram, indicating the load versus the vertebra deformation, can be accurately described with the aid of FEM–calculations using as simulation model of the cancellous bone, a network of struts possessing their real mechanical properties, surrounded by the cortical shell. This network has desired porosity in the cancellous bone region and a adjustable stiffness in vertical and horizontal directions.

2. EXPERIMENTAL SETUP OF THE VERTEBRAL BODY COMPRESSION TEST

The experimental setup used for the vertebrae compression test is shown in the upper part of Figure 1. The compression was performed between two rigid steel plates. Through the air pressure control of the upper steel plate driving piston and depending on the air supply, a force is exercised under a pre-adjusted growth rate. The force and the occurring displacement are simultaneously monitored. The corresponding displacement versus the load diagram is demonstrated in the bottom part of the figure. In this diagram three distinct areas are distinguished. In area I, the vertebra is compressed elastically up to a limit, where a fracture in the cortical shell region occurs. This fracture is characterized by the steep increase of the displacement in the diagram area II, at almost constant load. The further area III corresponds to the compression of the cancellous bone, since the cortical one is damaged and practically does not contribute to the vertebral rigidity in the compression direction.

A plot of the measured load F versus the occurring displacement h and versus the time t is presented in Figure 2. The applied load rate was kept constant as shown in the upper left of the F-t diagram. Even in the position of the cortical shell fracture, where a steep displacement took place (see bottom left diagram), the response of the compression piston was fast enough to keep the applied load rate practically constant. Photographs of the compressed vertebra are presented in the bottom right part of the Figure, corresponding to the indicated positions A, B and C in the F-h diagram.

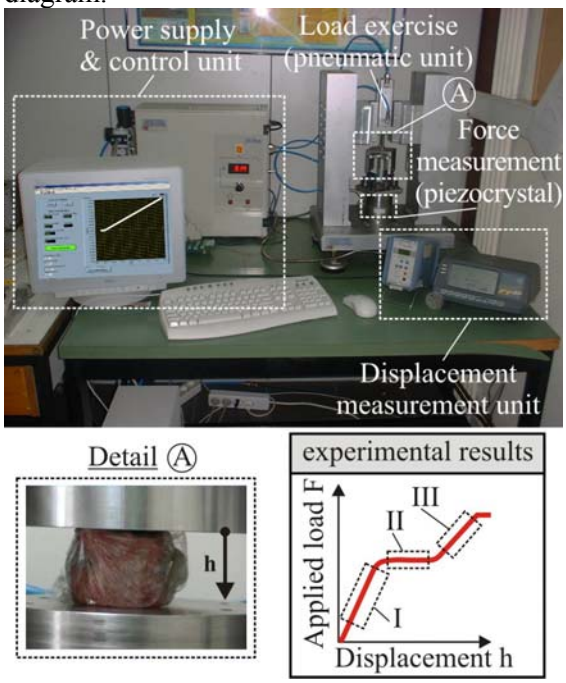

Figure 1: *Compression test experimental setup.*

3. NANOINDENTATION TEST TO DETERMINE TRABECULAR BONE STRUTS STRESS-STRAIN CURVES

Elastic properties of materials can be determined by means of nanoindentations [6,7] and corresponding instruments of high accuracy have been developed [8]. The pointed out references have to be considered as indicative, since a large number of related ones deal with these issues. In recent publications the "SSCUBONI" algorithm for the continuous

simulation of the nanoindentation was introduced, enabling the extraction of materials stress-strain elastic-plastic laws [3-5].

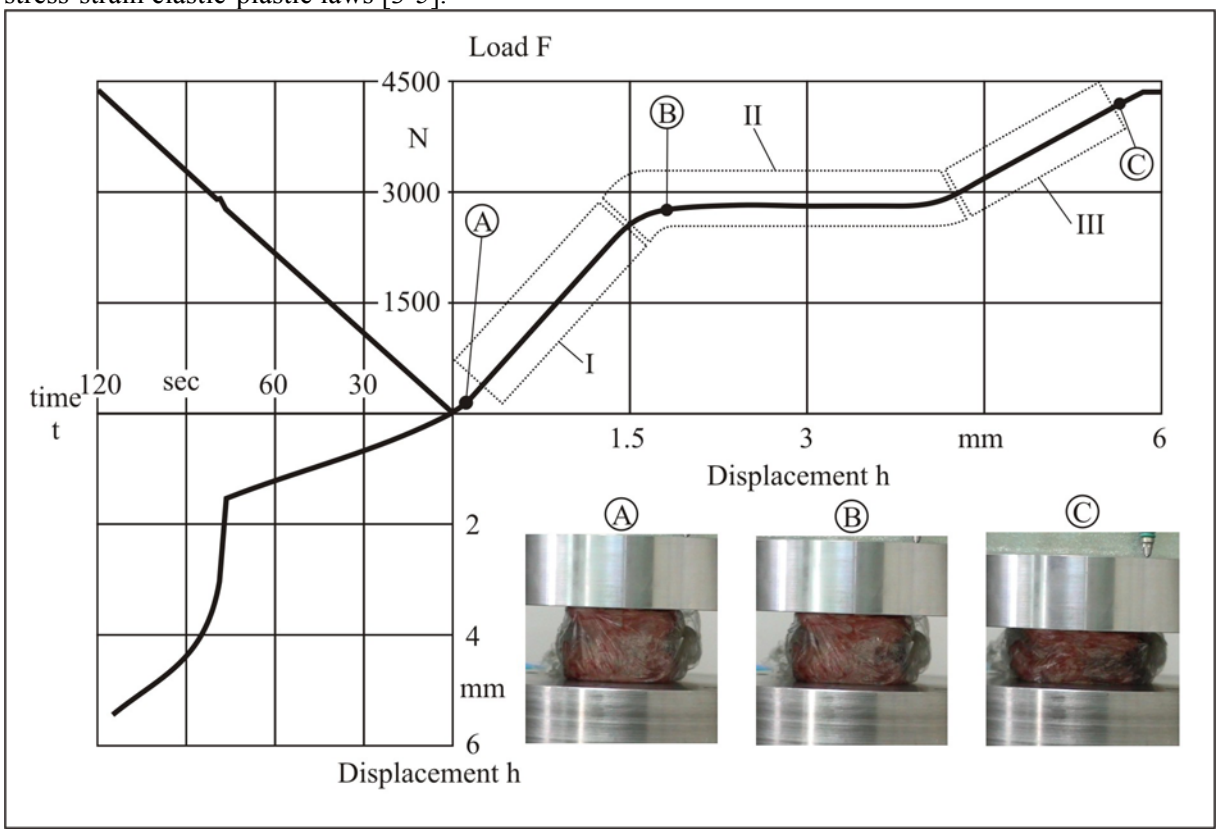

Figure 2: *Vertebra compression test experimental results.*

The used nanoindentation device in the frame of the described investigations is presented in Figure 3a. Nanoindentation is a precise procedure to continuously register the course of the applied force versus the occurring penetration depth. This measurement consists of two steps, the so-called loading stage and the unloading one (see Figure 3c). During the loading stage, an indentation load forces a diamond indenter to penetrate into the specimen. This load is gradually applied and at the same time the indentation depth is measured. When the load is fully removed, due to the resulting material plastic deformation, a remaining depth occurs, depending on the material properties as well as on the applied load and the indenter geometry.

A significant condition in nanoindentation evaluation procedures is the precise knowledge of the indenter tip geometry; since in nano-scale penetration depths, deviations from the ideal sharp tip geometry strongly affect the accuracy of the results [4,5]. These deviations were quantified in [4]. The continuous FEM simulation of the nanoindentation, due to accuracy reasons, is based on an axisymmetric FEM model of the semi-infinite material half space [3-5] as shown in Figure 3b. The associated boundary conditions and the finite elements discretisation network are explained in the details A and B respectively. In order to achieve a flexible and reproducible model, the indenter type and its tip geometry, the material properties as well as the penetration depth are variable and changeable parameters.

By means of the previously mentioned FEM model of the nanoindentation, as shown in the upper right part of the same Figure, the multi-linear constitutive law of trabecular bone struts, presented in Figure 3c, was determined. In this curve the elasticity modulus amounts to 13000 MPa, whereas the elasticity stress amounts to 60 MPa and the maximum stress to 94 MPa. These data represent the mean value of 700 measurements on individual lumbar spine trabecular bone struts.

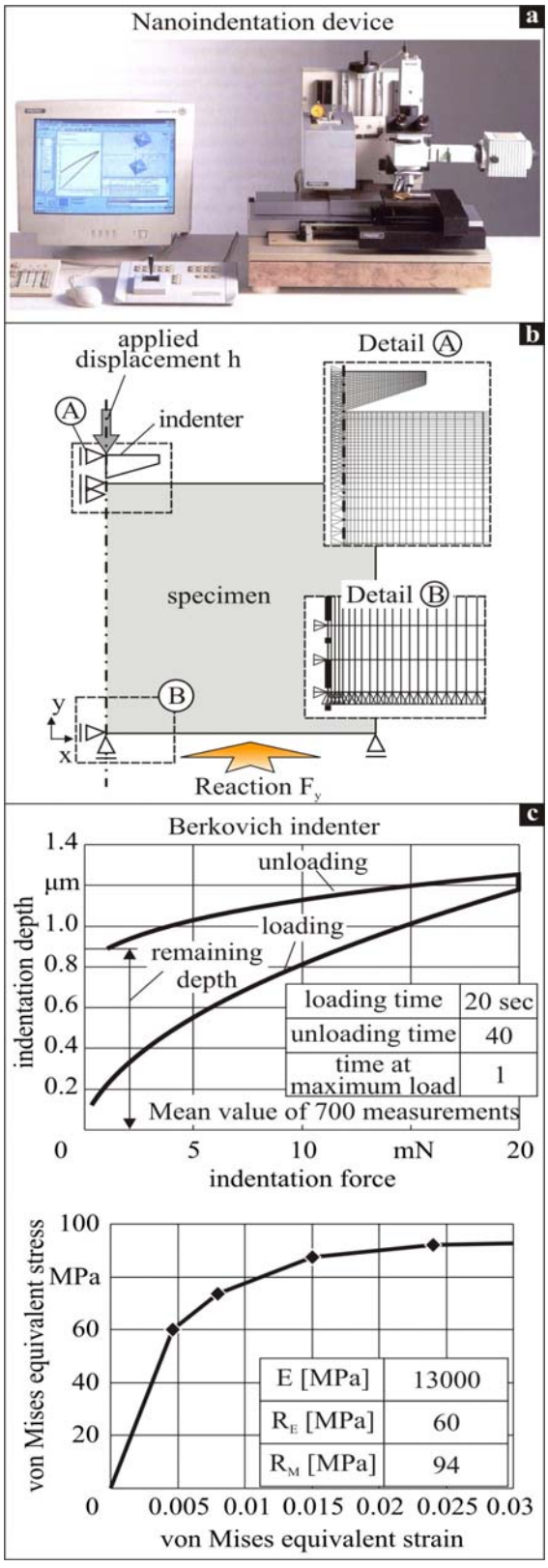

Figure 3: *Nanoindentation test and its FEM based algorithm to extract trabecular bone struts' stress-strain curves.*

4. FEM MODEL DESCRIBING THE COMPRESSION TEST USED TO EXTRACT BULK MECHANICAL STRENGTH PROPERTIES OF THE CANCELLOUS AND CORTICAL BONES

The examined L2 human vertebra, with the posterior elements removed and geometrical characteristics as the ones referred in [9-11], is presented in Figure 4a. In order to simulate this

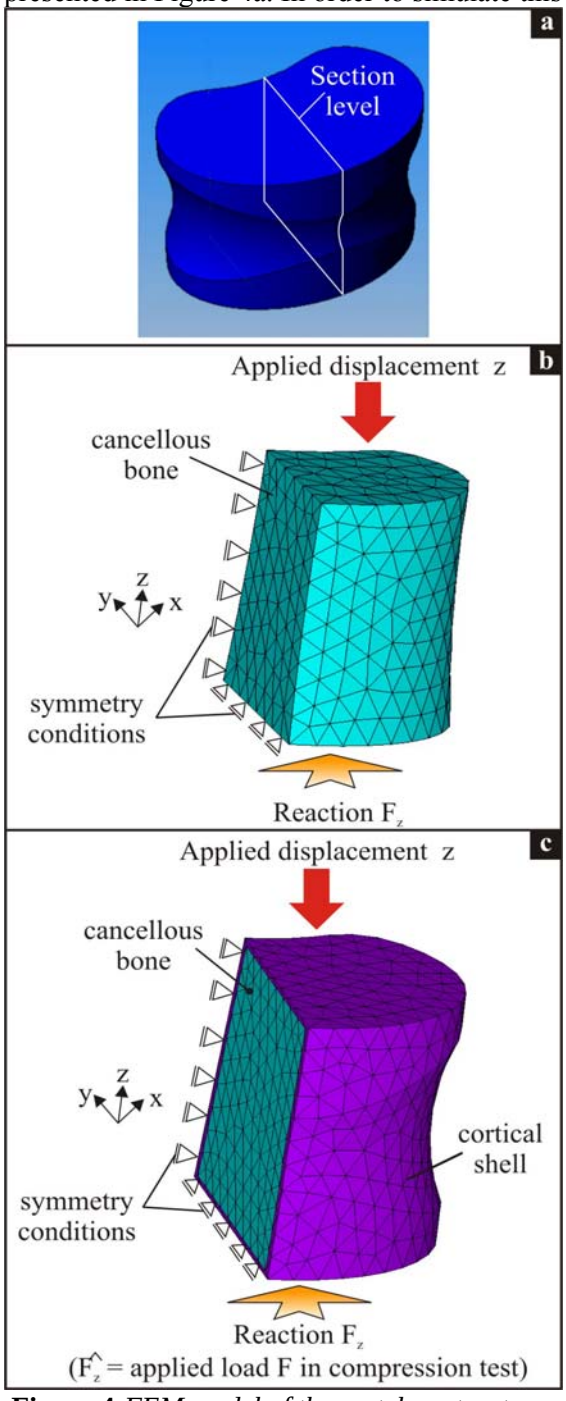

Figure 4:*FEM model of the vertebra structure.*

vertebra through a finite elements network and aiming to decrease the calculation time consumed, the half of the vertebra is considered, taking into account symmetry reasons (section A-A). The applied models in the evaluation procedures are illustrated in Figures 4b and c. Figure 4b represents the cancellous bone and figure 4c the cortical shell together with the cancellous. Both models were confined in their bottom faces to avoid movements in z-axis. In the upper face of each model a displacement h in the z-axis is applied and the resulting force in their bottom faces is determined.

As already described, the region III of the vertebra compression experimental diagram F-h (see Figure 1) mainly corresponds to the compression of the cancellous bone, since the cortical shell is already damaged at this test stage. On that account, the described in Figure 4 simulation model of the cancellous bone was applied to verify the course of region III of the experimental F-h diagram, as presented in the right part of Figure 5a. Assuming an elasticity modulus E and an elasticity stress S_E for the cancellous bone bulk material, an applied displacement leads to concrete reaction force, which is determined by means of FEM calculations. Through successive iterations, E and S_E values were discovered, verifying the experimental course in diagram region III. These values were 38 and 2.2 MPa for the elasticity modulus and stress respectively, which are in good agreement with published ones [11-13]. The occurring von Mises equivalent stress field is presented in the left part of Figure 5a, in the indicated position of

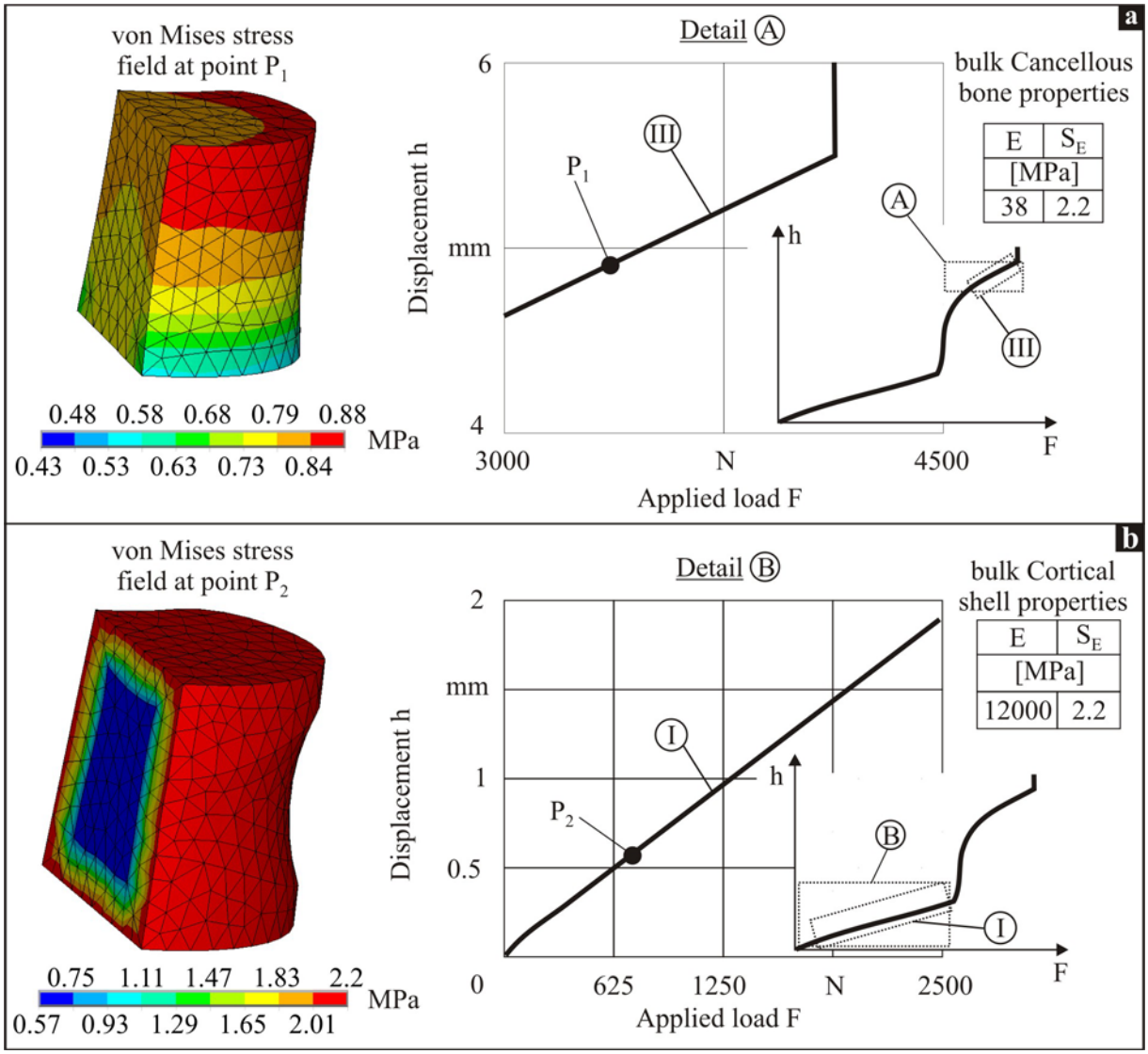

Figure 5. *Determination of apparent mechanical strength properties of cancellous bone and cortical shell materials.*

the diagram. Due to the existing geometrical and loading conditions the most stressed zone occurs in the external upper region of the cancellous bone.

In a second step, taking into account the previously deter-mined mechanical properties of the cancellous bone, the corresponding mechanical properties of the cortical shell are defined. Herein, the aim is to verify the course of the applied force F versus the occurring displacement h in the region I of the experimental F-h diagram (see detail B in right part of Figure 5b). Since the cancellous bone bulk elasticity modulus E and elasticity stress S_E were calculated in step 1, the corresponding data of the cortical bone have to be defined. By means of FEM supported iterative calculations using the previously mentioned model of the vertebra as a compound of the cancellous bone, surrounded by the cortical shell, these values were approximated to 12000 and 2.2 MPa for the modulus and stress of elasticity correspondingly, being in good agreement with the bibliography [14-16]. The resulting field stress is demonstrated in the left part of the Figure, verifying that the cortical shell breaks earlier in comparison to the core bone, since the maximum stress overriding the corresponding stress of elasticity appears in the external cortical shell region.

5. SUBSTITUTION OF THE CANCEL-LOUS BONE STRUCTURE WITH A NETWORK OF BEAM ELEMENTS WITH THE REAL MECHANICAL STRENGTH PROPERTIES OF THE TRABECULAR BONE STRUTS

The substitution of the spongy cancellous bone with a network of cylindrical beams in the vertebral body, having the mechanical strength properties determined by means of nanoindentation as illustrated in Figure 3, was conducted through an internal network of horizontal and vertical beam elements. The basic structure of this network corresponds to the structure of a reference cube (see Figure 6). The relation between the length of the horizontal beams to the corresponding one of the vertical beams, as well as the relations between their diameters are demonstrated in the same Figure according to the publications [18,22]. Moreover the cancellous bone trabecular struts network possesses different stiffnesses in horizontal and vertical directions [11,17-20] depending on the age [21,22].

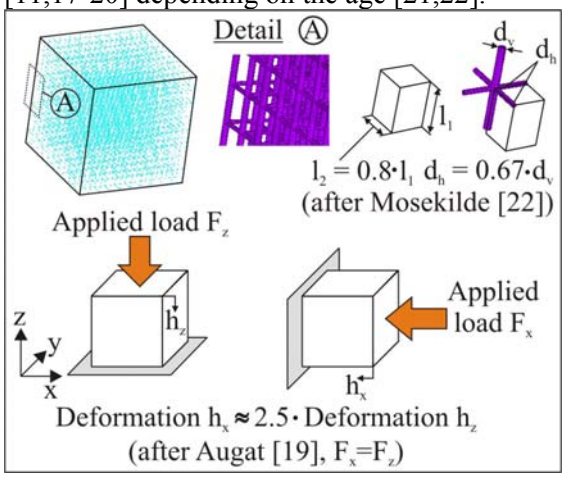

Figure 6: *Substitution of the cancellous bone structure with a network of cylindrical beams in the vertebral body, having strength anisotropy in the vertical and horizontal directions.*

According to Augat et al. [19], the vertebra deformation in horizontal loadings is increased in comparison to the corresponding one, when applying an equal vertical load (see Figure 6). Taking into account these facts, the size of the beams was calculated accordingly in order to achieve a percentage of 12% between the bone volume and the total volume (BV/TV) after Thomsen et al. [23].

Considering such a network of beams with geometrical characteristics previously described and mechanical properties, extracted by means of nanoindentations (see Figure 3), the bulk cancellous bone was replaced through this network in the examined vertebra geometry (see Figure 7). The cortical bone mechanical properties are equal to the ones determined in Figure 4. A simulation of the vertebra compression with the cancellous bone replaced by an appropriate network of beams, leads to an adequate verification of the experimental F-h diagram, shown in Figure 2.

6. CONCLUSIONS

Stress-strain curves of trabecular bone struts were determined by means of nanoindentations and an appropriate FEM-based evaluation algorithm. Beforehand the cortical and cancellous bones' bulk mechanical properties were determined by means of a

compression test on an L2 human vertebra and appropriate FEM models. The herein determined bulk mechanical properties were in good agreement with corresponding ones presented in bibliography.

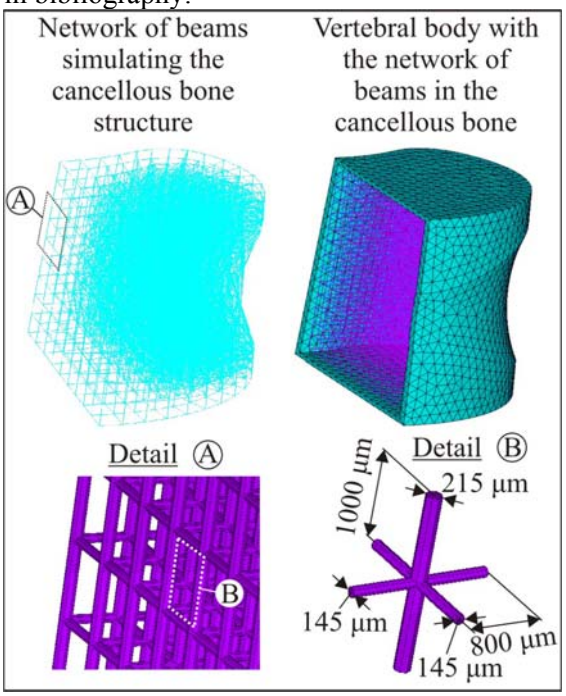

Figure 7: *Simulation of the vertebral body considering a network of beams, describing the cancellous bone.*

The stress-strain curves determined by means of nanoindentations were applied to describe the mechanical strength properties of beam elements, which replaced the cancellous bone material structure. The corresponding network was built by means of horizontal and vertical beams, having a predefined BV/TV ratio and different stiffness when loaded horizontally and vertically. The application of a network with such geometrical characteristics and mechanical properties, simulating the vertebra cancellous core, lead to a sufficient analytical description of the vertebra compression test.

7. REFERENCES

[1]. Liebschner M, Kopperdahl D, Rosenberg W, Keaveny T. Finite element modeling of the human thoracolumbar spine. Spine, 2003, 559-565.

[2]. Ebbesen EN, Thomsen JS, Beck-Nielsen H, Nepper- Rasmussen HJ, Mosekilde L. Lumbar vertebral body compressive strength evaluated by dual-energy X-ray absorptiometry, quantitative computed tomography and ashing. Bone 1999; 25(6):713-724.

[3]. Bouzakis K-D, Michailidis N, Erkens G. Thin hard coatings stress-strain curves determination through a FEM supported evaluation of nanohardness results. Surface and Coatings Technology 2001; 142-144:102-109.

[4]. Bouzakis K–D, Michailidis N, Hadjiyiannis S, Skordaris G, Erkens G. A continuous FEM simulation of the nanoindentation to determine actual indenter tip geometries, elastic-plastic material deformation laws and universal hardness. Zeitschrift fuer Metallkunde 2002; 93:862-869.

[5]. Bouzakis K–D, Michailidis N, Hadjiyiannis S, Skordaris G, Erkens G. The effect of specimen roughness and indenter tip geometry on the determination accuracy of thin hard coatings stress-strain laws by nanoindentation. J Mater Characterisation 2003; 49:149-156.

[6]. Oliver WC, and Pharr GM. An improved technique for determining hardness and elastic modulus using load and displacement sensing indentation experiments. J Mater Res 1992; 7:1564-1583.

[7]. Alcala J, Giannakopoulos AE, and Suresh S, Continuous measurements of load-penetration curves with spherical microindenters and the estimation of mechanical properties, J Mater Res 1998; 13:1390-1400.

[8]. HELMUT FISCHER. GmbH +Co Evaluation Manual of Indentation Procedure. Sindelfingen-Germany, 2000.

[9]. Panjabi MM, Goel V, Oxland T, Takata K, Duranceau J, Krag M, Price M. Human lumbar vertebrae quantitative three-dimensional anatomy Spine, 1992; 17(3):299-306.

[10]. Edwards T, Yinggang Z, Lisa F, Hansen Y. Structural Features and Thickness of the Vertebral Cortex in the Thoracolumbar Spine. Spine, 2001; 26(2):218-225.

[11]. White A, Panjabi MM. Clinical biomechanics of the spine, 2nd edition. Lippincott Williams & Wilkins Publishers, Hagerstown MD USA;1990.

[12]. Lindahl O, Mechanical properties of dried defatted spongy bone. Acta Orthop Scand 1976; 47:11-19.

[13]. Hanson TH, Keller TS, Panjabi MM, A study of the compressive properties of lumbar vertebral trabeculae: effects of tissue characteristics. Spine 1987, 12:56-62.

[14]. Skalli W, Robin S, Lavaste F, Dubousset J. A biomechanical analysis of short segment spinal fixation using a 3-D geometric and mechanical model. Spine 1993; 18:536-545.

[15]. Goel VK, Kim YE, Lim TH, Wibstein JN. An analytical investigation of mechanics of spinal instrumentation. Spine 1988; 13:1003-1011.

[16]. Shirazi A, Shrivastava SC, Ahmed AM. Stress analysis of the lumbar disc-body unit in compression: a three-dimensional nonlinear finite element study. Spine 1984; 9:120-134.

[17]. Ulrich D, van Rietbergen B, Weinans H, Rógsegger P. Finite element analysis of trabecular bone structure: a comparison of image-based meshing techniques. J Biomech 1998; 31:1187-1192.

[18]. Kim HS, Al-Hassani STS. A morphological model of ver-tebral trabecular bone J Biomech 2002; 35:1101-1114.

[19]. Augat P, Link T, Lang TF, Lin JC, Majumdar S, Genant HK. Anisotropy of the elastic modulus of trabecular bone specimens from different anatomical locations. Med Eng Phys 1998; 20:124–131.

[20]. Cortet B, Marchandise X. Bone microarchitecture and mechanical resistance. Joint Bone Spine, 2001; 68:297-305.

[21]. Thomsen JS, Ebbesen EN, Mosekilde L. Age-related differences between thinning of horizontal and vertical trabeculae in human lumbar bone as assessed by a new computerized method. Bone 2002; 31:136–142.

[22]. Mosekilde L. Age-related changes in vertebral trabecular bone architecture-assessed by a new method. Bone 1988; 9:247-250.

[23]. Thomsen JS, Ebbesen EN, Mosekilde L. A new method of comprehensive staic histomorphometry applied on human lumbar vertebral cancellous bone Bone 2000; 27:129–138.